The new Swiss Glacier Inventory SGI2010: relevance of using high-resolution source data in areas dominated by very small glaciers

Mauro Fischer†*
*Matthias Huss**
Chloé Barboux and*
*Martin Hoelzle**

*Department of Geosciences, University of Fribourg, Chemin du Musée 4, CH–1700 Fribourg, Switzerland
†Corresponding author: mauro.fischer@unifr.ch

Abstract

In view of the rapid and accelerating glacier retreat observed in the European Alps during the last decades, the repeated creation of glacier inventories is important to understand the spatio-temporal variability of glacier changes and to support modeling studies. This article presents the latest glacier inventory for the entire Swiss Alps (SGI2010) derived by manual digitization from high-resolution (25 cm) aerial orthophotographs acquired between 2008 and 2011. Its accuracy is assessed by comparing the extents of clean, snow- and/or debris-covered glaciers derived from multiple digitization by several experts. The potential of more precise mapping of debris-covered glaciers is pointed out through the combination of aerial orthophotos with Differential Synthetic Aperture Radar Interferometry (DInSAR) techniques. In order to investigate the accuracy of glacier outlines obtained from medium-resolution satellite remote sensing imagery, a Landsat derived 2003 inventory is directly compared to all glaciers of the eastern Swiss Alps mapped with 2003 aerial orthoimagery. For the Swiss Alps, the total glacierized area mapped for 2010 is 944.3 ±24.1 km^2. Resulting area changes are -362.6 km^2 (-27.7%, or -0.75% a^{-1}) between 1973 and 2010. It is shown that satellite remote sensing techniques using medium-resolution source data misclassified more than 25% in area of very small glaciers (<0.5 km^2). Therefore, use of high-resolution satellite or airborne imagery for future inventory creation in areas dominated by very small glaciers is recommended.

Introduction

Observed fluctuations of mountain glaciers are known to be among the best indicators of climate change (e.g., IPCC, 2013). Continuous glacier monitoring is thus crucial and must include the repeated creation of glacier inventories (Haeberli, 2004) in order to understand observed glacier changes and project their future evolution (e.g., Hoelzle et al., 2007; Abermann et al., 2009; Huss, 2012). Furthermore, updated inventories are essential for assessing climate change impacts on future runoff in glacierized catchments (e.g., Huss, 2011; Sorg et al., 2012).

For the European Alps, mapped glacier outlines are stored in regional or national inventories. They are available for different acquisition dates and result from different methods (automatic or semi-automatic approaches, manual digitization) and data sources (satellite data, aerial photography, laser scanning, topographic maps) (e.g., Paul et al., 2002; Lambrecht and Kuhn, 2007; Knoll and Kerschner, 2009; Abermann et al., 2010; Carturan et al., 2013). Based on a set of Landsat Thematic Mapper (TM) scenes (30 m resolution) acquired in autumn 2003 and a semi-automated approach, Paul et al. (2011) were the first to map the extents of glaciers in the entire European Alps spatio-temporally consistently. For the Swiss Alps, the latest glacier outlines prior to the inventory presented here originate from that study.

The rapid mass loss and shrinkage of Alpine glaciers observed during the past years (e.g., Zemp et al., 2008, 2012, 2013) requires more frequent updates of glacier inventories (every 5-10 years; Paul et al., 2007). The 2003 outlines are thus already outdated for the Swiss Alps. Moreover, the spatial resolution of the source data used for creation of the 2003 inventory might be too poor for the assessment of specific questions on smaller scales. Using medium-resolution (e.g., Landsat, ASTER) satellite imagery has indeed become the state-of-the-art for creating new glacier inventories for remote areas (cf. Raup et al., 2007; Bolch et al., 2010; Andreassen and Winsvold, 2012; Frey et al., 2012; Falaschi et al., 2013; Nuth et al., 2013). If medium-resolution source data are used, however, the accuracy of such methods is rather limited for investigating changes in very small glaciers (Paul et al., 2013), here defined according to Huss (2010) as being smaller than 0.5 km^2. This is problematic because very small glaciers are numerous in most glacierized areas around the world and can even play a role for the accuracy of global glacier change assessments (Bahr and Radić, 2012).

Hence, trying to understand the peculiarities and the response of glaciers in the Swiss Alps to climate change asks for as accurate as possible glacier outlines. Using high-resolution air- or spaceborne imagery helps to overcome the potential shortcomings of medium-resolution source data for the delineation of glacier boundaries (cf. DeBeer and Sharp, 2009). Therefore, the 50/25 cm resolution aerial orthoimagery available for the entire Swiss Alps since the late 1990s from the Swiss Federal Office of Topography (swisstopo) is highly valuable source data for glacier mapping.

In this article we present the new Swiss Glacier Inventory (SGI2010) derived from manual delineation of glacier outlines based on aerial orthoimagery acquired between 2008 and 2011. The source data used for its creation and the chosen methodological approaches are described in detail. Further, some selected aspects of glacier change assessment are shown. The accuracy of our inventory is evaluated by comparing glacier outlines for clean, snow- and/or debris-covered glacier boundaries from multiple digitization by different experts. Glacier outlines for the eastern Swiss

Alps are also delineated from aerial orthophotographs of 2003. Direct comparison to the 2003 inventory compiled by Paul et al. (2011) allows a detailed evaluation of the accuracy of glacier outlines derived from medium-resolution satellite imagery. Furthermore, the combination of Differential Synthetic Aperture Radar Interferometry (DInSAR) with airborne orthophotography is tested. We show the potential of this promising technique to refine and assess the accuracy of glacier outlines over debris-covered areas.

Study Region

In the Swiss Alps, prevailing climatological and topographical boundary conditions lead to a clear asymmetry of the glacierization between the western and eastern part. Western Switzerland is strongly glacierized with large areas of potential snow and ice accumulation along the high-altitude northern Alpine crest (Bernese Alps) and the main Alpine crest (Valais Alps) (Maisch et al., 2000). Overall, the sample of glaciers in Switzerland is dominated by small and rather steep glaciers. Firn or ice patches and glacierets are the most common and widespread glacier types (Haeberli and Hoelzle, 1995). Larger mountain and valley glaciers are outnumbered but account by far for the largest part of the glacierized area and the ice volume (cf. Farinotti et al., 2009).

Glaciers in the Swiss Alps generally reached their Little Ice Age (LIA) maximum extent around 1850 (Ivy-Ochs et al., 2009). For this time the reconstructed total glacierized area is 1735 km^2 (Maisch et al., 2000). In the following, glaciers showed general retreat. In 1973, 1307 km^2 were still covered by glaciers, which corresponds to a total area loss of 428 km^2 (–25%, or –0.2% a^{-1}) between the LIA maximum and 1973. After a stagnant phase during the 1970s to the mid-1980s with only minor area changes, glaciers in the Swiss Alps rapidly retreated again (–18%, or –1.3% a^{-1} from 1985 to 1999) (Paul et al., 2004) and showed considerable surface elevation and mass changes (Fischer et al., 2014).

Data Sets

The study area covers the entire Swiss Alps. The reference year for our inventory is 2010 as most entities are mapped from source data acquired in autumn 2010 (Fig. 1). Accordingly, it is hereafter referred to as the Swiss Glacier Inventory 2010 (SGI2010). For area change assessments, comparative analyses and the accuracy assess-

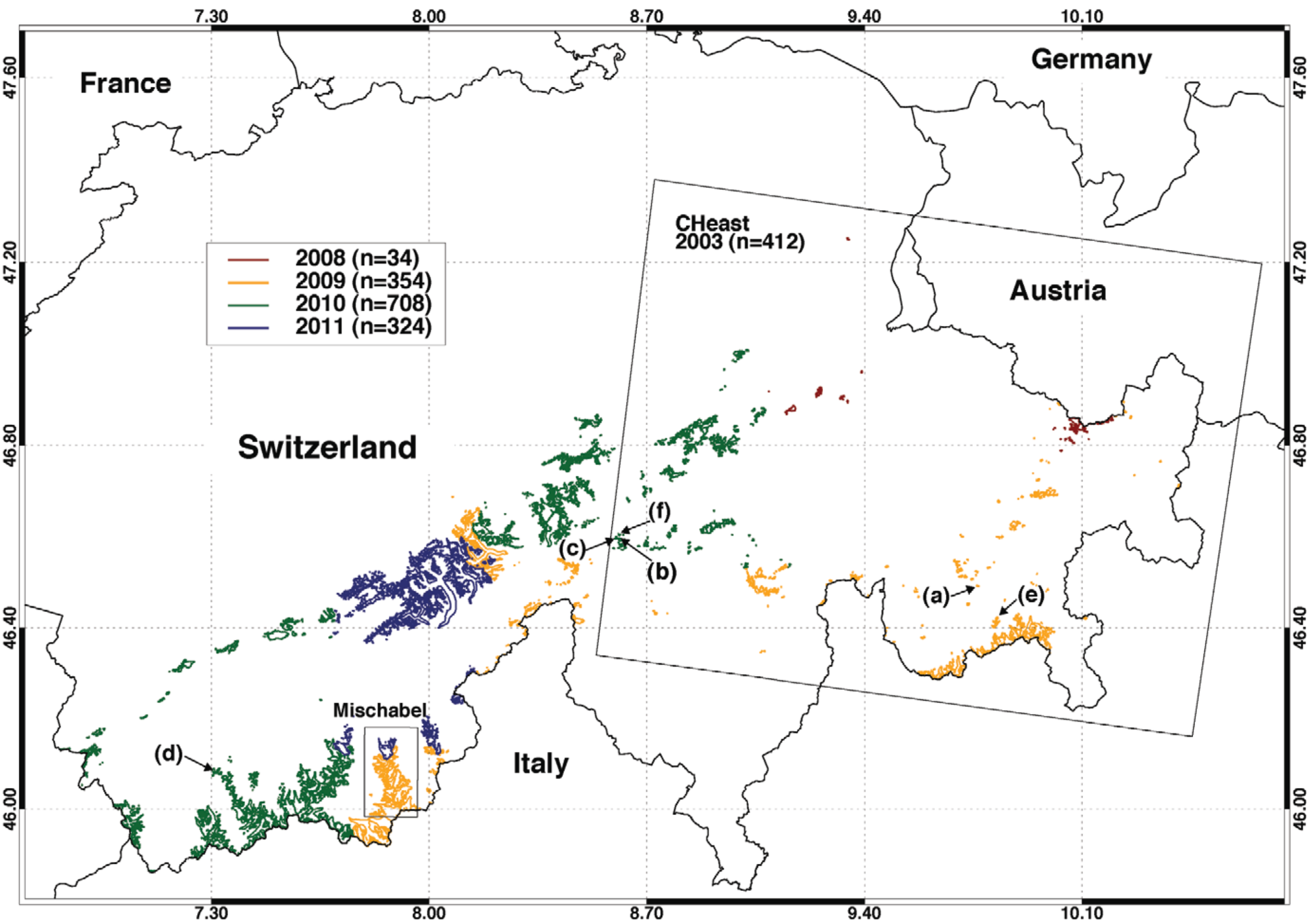

FIGURE 1. Glaciers in the Swiss Alps by 2010. Colors refer to the year of the aerial orthophotography tile(s) used for glacier mapping. The number of glacier entities mapped for the respective year is given in parentheses. The locations of six very small glaciers chosen for accuracy assessment are indicated with (a) to (f). The small rectangle shows the subsample of glaciers within the Mischabel area used to test the potential refinement of glacier outlines with Differential Synthetic Aperture Radar Interferometry (DInSAR) coherence images. The large rectangle contains glaciers in the eastern Swiss Alps, which were also mapped with orthoimagery of 2003.

ment of the applied method, the following two (out of four) former Swiss glacier inventories are used: (1) the Swiss Glacier Inventory 1973 (Müller et al., 1976) was derived from stereo-photogrammetry-based interpretation of aerial photography data collected in early September 1973. Maisch et al. (2000) compiled and completed the data set for the entire Swiss Alps, and Paul (2004) provided it in finalized digital format. (2) The 2003 inventory was derived with a semi-automated method applying a threshold ratio of spectral bands (TM 3/5) to extract glacier outlines from Landsat TM scenes acquired between the 6 and 13 August 2003 (Paul et al., 2011).

In order to compare the SGI2010 to the 2003 inventory, the subsample of all glaciers in the eastern Swiss Alps (412 entities in 2003; see large rectangle in Fig. 1) is mapped twice, once based on aerial orthophotographs of the SWISSIMAGE Level 1 mosaic recorded in autumn 2003 and once based on most recent orthoimagery of the SWISSIMAGE Level 2 data set (recorded mostly in 2009 for this area). The SWISSIMAGE Level 1 mosaic consists of analog aerial imagery that was scanned and orthorectified with a ground resolution of 50 cm (swisstopo, 2010). The SWISSIMAGE Level 2 mosaic is the main source data used for the creation of the SGI2010 and is composed of high-resolution (25 cm) digital aerial orthophotographs covering entire Switzerland. Images were taken on cloudless days and at the end of the ablation season (September/October) with a Leica ADS80 digital camera onboard a Super King Air 350C or a Twin Otter DHC-6-3000 flying at an operating altitude of about 5000 m a.s.l. over mountain areas. The positional accuracy is ±3–5 m in the area of interest. Individual images are georeferenced in the LV95 reference system by means of aerotriangulation and orthorectified by projection onto the DHM25 (swisstopo, 2010). Detailed analyses of the individual 2003 and 2008–2011 SWISSIMAGE tiles used for glacier mapping revealed that the vast majority of glacier-adjacent areas were completely free of seasonal snow cover up to the highest mountain peaks, and transient snowlines on glaciers were comparatively very high at the time of the aerial surveys. This is due to the 2003 summer heat wave and the particularly warm summers/autumns 2008–2011 with only rare snowfall events (cf. Glaciological Reports, 2011–2014), and was—together with the absence of clouds on the aerial orthoimagery—in favor of accurate glacier mapping.

For issues concerning the recent glacier surface topography, the new 2 m resolution digital elevation model (DEM) of entire Switzerland, swissALTI^{3D}, is used. For areas above 2000 m a.s.l. (i.e., for nearly all of the currently glacierized areas), the data set was accomplished by stereocorrelation of 2008–2011 SWISSIMAGE Level 2 aerial orthoimagery (swisstopo, 2013). The combination of 2008–2011 SWISSIMAGE Level 2 and most recent swissALTI^{3D} data is ideal to create a new glacier inventory because their acquisition dates are identical.

Methods

MAPPING GLACIER OUTLINES

All glacier outlines of the SGI2010 were manually digitized in ArcGIS based on corresponding SWISSIMAGE Level 2 tiles. Because 98% of the source data was acquired over only two hydrological years (autumn 2009 to autumn 2011) and the deviations in glacier extent from the reference year 2010 are assumed to cancel each other out for all glaciers (Fig. 1), the inventory was not temporally homogenized. To ensure data consistency, mapping was carried out by only one single expert (Mauro Fischer, University of Fribourg). The total working time to complete the inventory roughly amounted to four months.

Previous inventories are very helpful to delineate new glacier outlines (Paul et al., 2011). In this study we used the digital extents of the 1973 inventory as a reference or starting point in order not to miss any glacierized surfaces. Moreover, we adopted the 1973 coding scheme designed based on a hydrological classification (cf. Maisch et al., 2000). Mapped glacier polygons were strictly coded and named according to the 1973 outlines they fell into or overlapped with. This allowed a glacier-individual change assessment. For hydrological drainage divides usually found in the accumulation area and at high altitude, the 1973 outlines were traced during digitization, unless a distinct surface lowering with its corresponding change in the ice surface topography was clearly visible from the orthophotographs. In these rather rare cases, new drainage divides were manually drawn with the help of the most recent topographic map or a hillshade of the respective area created from the high-resolution swissALTI^{3D} DEM.

The character of the periglacial environment in the proximate surroundings of the glacier margins influenced the accuracy of, as well as the time per area to digitize individual glacier polygons. The latter ranged from less than a few minutes to more than one hour. Generally, four situations occurred: (1) very distinct glacier margins where bare ice meets solid bedrock. Such outlines were easy to map, the accuracy was high, and the digitizing time reduced to a minimum (Fig. 2, part a). (2) Less clear glacier outlines where marginal areas are to a large extent debris-covered and/or adjacent areas are made up of a recently uncovered sediment bed, lateral moraine, or buried glacier ice. For such situations, a thorough interpretation of glacier boundaries was not always straightforward and could result in error-prone outlines in the worst-case (cf. snout of Innre Baltschiedergletscher in Fig. 2, part b). However, the presence of crevasses and/or exposed ice as well as abrupt changes in the surface topography helped to better delineate glacier boundaries over debris-covered areas. (3) Less distinct glacier outlines where the transition between snow-covered glacier surface and seasonal and/or perennial snowfields is ambiguous. Due to the very favorable snow conditions on the aerial orthophotographs used, this situation only occurred in rare cases, for instance if small seasonal or perennial snow patches were found within the 1973 outlines and the current (2010) glacier extents. Visible rock and/or debris surface helped to define glacier margins in such situations. Figure 2, part c, can be seen as a worst-case example encountered. (4) Less clear glacier outlines in very shadowy areas, for instance, steep north-facing headwalls. This was hardly ever an issue because the SWISSIMAGE orthophotos used were of high resolution and quality. Having shadowy areas increased digitizing time per area to a certain extent but did not directly affect the accuracy of the digitized outlines (Fig. 2, part d).

GLACIER INVENTORY PARAMETERS

We followed the World Glacier Monitoring Service (WGMS) "guidelines for the compilation of glacier inventory data from digital sources" version 1.0 (Paul et al., 2009) to derive the parameters for individual glaciers inventoried in the new SGI2010 database. The latter comprise the following: (1) identification (ID) according to the hydrological coding of the 1973 inventory (cf. Maisch et al., 2000); (2) x- and y-point coordinates, ideally of the upper part of the ablation area and close to the central flowline; (3) acquisition date of the SWISSIMAGE tiles used; (4) surface area (km^2); (5) length (km); (6) minimum, (7) maximum, (8) mean, and (9) median elevation (m a.s.l.); (10) mean slope (degree); and (11) mean aspect divided into eight classes. The parameters 6–10 were

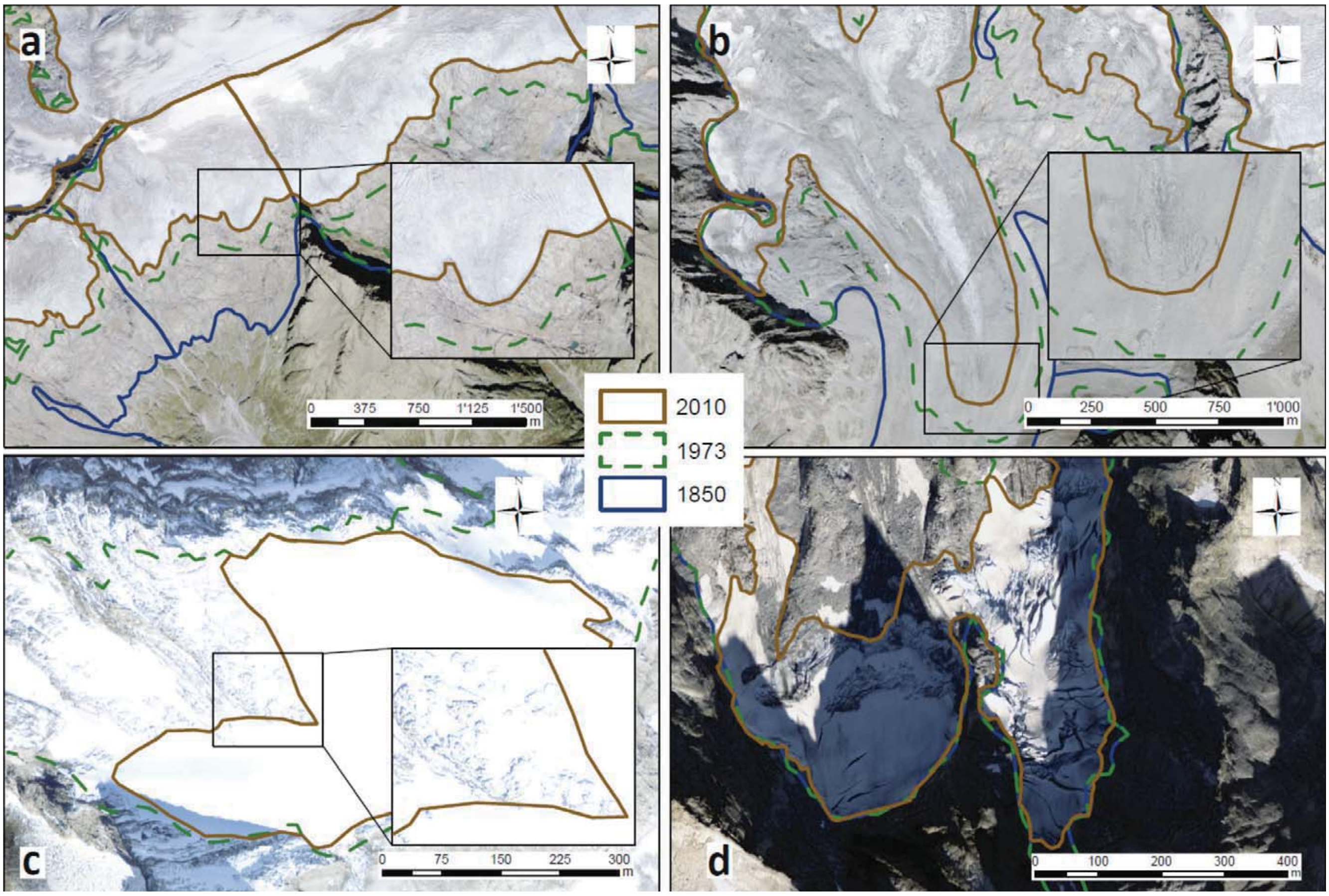

FIGURE 2. Examples of different situations encountered when mapping glacier outlines: (a) bare ice meets solid bedrock (Tellingletscher, 2011); (b) debris-covered marginal zones (Innre Baltschiedergletscher, 2011); (c) snow-covered marginal zones (Bächistockfirn, 2010); and (d) shadowy areas (Vadrec da la Trubinasca-E, 2009). Digitized outlines from 1850 (navy blue), 1973 (dashed green), and 2010 (brown) are overlain to the respective SWISSIMAGE orthophoto tile based on which the latest outline was drawn.

calculated by combination of the SGI2010 outlines with the 2 m swissALTI^{3D} DEM. Glacier length (parameter 5) was measured along an automatically derived center line (cf. Machguth and Huss, 2014). The entire data set is available over the Global Land Ice Measurements from Space (GLIMS) database.

ACCURACY OF MAPPED GLACIER OUTLINES

Assessing the accuracy of glacier outlines derived by any of the known methods (manual digitizing, semi-automatic satellite remote sensing approaches, algorithms applied to high-resolution DEMs, etc.) is not straightforward and often difficult. This is mainly because systematic reference data—for instance, from differential GPS—independent from the source data of the outline is lacking (Racoviteanu et al., 2009), or only available/feasible to be collected for a small number of selected glaciers (e.g., Diolaiuti et al., 2012).

As a complete data set of higher resolution than the source data used here was not available, the accuracy of the mapped glacier outlines could not be validated in sensu stricto. Thus, following the recommendations by Paul et al. (2013), we performed an accuracy assessment based on a "round robin" experiment with nine expert participants. Providing them with selected orthophotographs containing clean, debris-covered, snow-covered, and shadowy glacier boundary areas, we obtained multiple individual digitizations of the same glacier entities for each of the so-called "critical boundary situations" (see Fig. 2). We merely chose small glaciers for this assessment because the potential relative error in glacier mapping strongly increases with decreasing glacier surface area (Paul et al., 2013) and the glacier-size distribution in the European Alps is dominated by small glaciers. Also, we were able to quantify the accuracy of mapping larger glaciers by comparison to inventory data from medium-resolution satellite imagery (cf. accuracy assessment section in discussion chapter below).

MAPPING DEBRIS-COVERED GLACIERS USING DInSAR AND AIRBORNE PHOTOGRAPHY

Despite the high quality, resolution, and level of detail visible on the SWISSIMAGE orthophotographs, correct mapping of debris-covered glaciers or boundary areas was most problematic. This has been confirmed in a number of previous studies, applying both automatic and manual glacier mapping techniques (e.g., Knoll and Kerschner, 2009; Diolaiuti et al., 2012; Falaschi et al., 2013). Frey et al. (2012) showed that debris-covered glaciers could be delimited using the coherence of interferograms from radar images. Therefore, we investigated the potential of combining DInSAR with airborne photography data for more accurate mapping of debris-covered glaciers.

DInSAR is known as a well-established technique for mapping surface displacement at high spatio-temporal resolution (e.g., Massonnet and Feigl, 1998). The nature of the reflected microwave signal response depends on sensor parameters (wavelength, polarization, system noise, etc.), on the imaging geometry (interferometric baseline, local incidence angle), and on target parameters (composition and surface roughness of the ground). The former two can mostly be identified as such during interferometric processing (Atwood et al., 2010; Strozzi et al., 2010). If backscatter properties change between two consecutive image acquisitions, there is a loss of coherence between the SAR scenes used for interferometry (Klees and Massonnet, 1999). This phenomenon of decorrelation is expressed as a noise with contrasted colors of neighboring pixels on the interferogram. It can be measured by means of local correlation, yielding a normalized coherence of the individual pixels. During wintertime, dry snow preserves stable scattering geometries, allowing high degrees of coherence and uniform colors on DInSAR interferograms. On the other hand, melting snow or wet ice causes changes of the scattering geometries and thus strong decorrelation and noise (Strozzi et al., 1999). A significant glacier motion (decimeters to meters per day) implies a strong glacier surface deformation and low coherence (Weydahl, 2001). For debris-covered glaciers, a decorrelated signal is either caused by glacier motion, by exposure of the melting ice itself (thinner debris-coverage), and/or by the rapid settlement of the glacier surface (Delaloye et al., 2007).

For a representative subsample of 48 glaciers of all size classes and surface types in the Mischabel area (Fig. 1), we compared the SGI2010 outlines from manual digitization with coherence images from 10 selected TerraSAR-X (TSX) DInSAR pairs (5 in descending and 5 in ascending mode) with 11 days time lapse of the summers 2008–2012. DInSAR interferograms were processed with the commercial software GAMMA in the two-pass approach using the 2 m resolution swissALTI^{3D} DEM resampled to 5 m pixel spacing. Coherence images were derived for all scene pairs applying the following workflow: (1) pixels with a measured coherence below 0.8 were classified as noisy, and as stable otherwise, and (2) the resulting pixels on the coherence images were classified by the most represented class of the five selected pairs.

Results

CHANGES IN AREA AND NUMBER 1973–2010

Over the entire Swiss Alps, the total glacierized area mapped for 2010 is 944.3 km^2 (2.3% of the total area of Switzerland). This corresponds to a total area loss of 27.7% since 1973 (1306.9 km^2 covered by glaciers). In number, 1420 individual glacier entities (which may consist of more than one outline) remain by 2010 and 733 glaciers (34%) have completely vanished since 1973. Relative changes in area for individual size classes are highest for glaciers <1.0 km^2 and lowest for medium-sized glaciers (5.0–10.0 km^2) compared to 1973. The percentaged size-class distribution has only slightly changed since 1973 (Table 1). Very small glaciers still dominate in terms of total number, but the vast majority of the glacierized area belongs to medium and large glaciers. Nevertheless, a general trend of amplification of this relation since 1973 is obvious. Comparatively, more glacierized area belongs to fewer glacier entities and vice versa (Table 1, see also Fig. 3, parts a and b). While for glacier size classes <5.0 km^2 the percentage of the total glacierized area decreased, glaciers larger than 5.0 km^2 proportionally account for even more of the presently still existing ice than in 1973 (Fig. 3, part a). In terms of the relative number of glaciers (Fig. 3, part b), there is a significant increase of the smallest size class (<0.1 km^2) and a slight increase of size classes >1.0 km^2, whereas the number of individual entities decreased for glaciers >0.1 km^2 and <1.0 km^2. This demonstrates that medium to large glaciers (>1.0 km^2) did not disappear at all (Fig 3, part c), but might have been shifted into a smaller size class. Hence, with exception of the smallest class, the numeric predominance of glaciers <1.0 km^2 decreased to a certain extent.

TABLE 1

Changes in area and number of glaciers between 1973 and 2010 evaluated for different size classes.

Size class (km^2)	1973 count	1973 area (km^2)	2010 count	2010 area (km^2)	Area change 1973–2010 (km^2)
<0.1	1058	42.3	770	25.3	–17.0
0.1–0.5	715	162.1	396	93.0	–69.1
0.5–1.0	162	110.3	91	65.4	–44.9
1.0–5.0	167	321.6	118	225.3	–96.3
5.0–10.0	33	233.5	29	196.7	–36.8
>10.0	20	437.1	16	338.6	–98.5
Total	2155	1306.9	1420	944.3	–362.6

Relative changes in glacier area between 1973 and 2010 vary significantly for individual glaciers (Fig. 3, part c). Nevertheless, the scatter drastically increases toward smaller glacier size classes. Many very small glaciers completely vanished, while others did not show significant areal shrinkage. There is a general trend of decreasing relative area changes with increasing initial glacier size in 1973 (Fig. 3, part c).

In both 1973 and 2010, most of the glacierized area in the Swiss Alps belongs to north-facing glaciers (mean aspects NW-N-NE, 59.4% [1973] and 58.2% [2010] of the total glacierized area) (Fig. 3, part d). The mean aspect class SE is not representative because it is strongly influenced by Grosser Aletschgletscher, the largest glacier of the European Alps (78.4 km^2 in 2010). Relative changes in area and number are smallest for SE-exposed (–18.7% in area, –18.2% in number) and highest for W-exposed glaciers (–36.1% in area, –42.5% in number). This can be explained by the different sensitivity to changes in air temperature increase for the respective aspect classes (cf. Evans and Cox, 2005; Evans, 2006): due to the relatively higher influence of the shortwave radiation component, south-exposed glaciers generally react less sensitive to air temperature changes than more north-exposed glaciers. Furthermore, south-exposed glaciers are often smaller. Therefore, their response time is shorter and mass balance less negative, which in turn can explain the smaller changes in area and number.

ACCURACY OF MAPPED GLACIER OUTLINES

The overlays of glacier outlines resulting from multiple digitization were highly consistently delineated by all experts where bare ice or snow-covered ice meets bare bedrock, due to the high resolution of the orthoimages even in cast shadow (different outlines lie within 3 to 30 m, Fig. 4, part a). Where glacier-adjacent areas consisted of a recently uncovered sediment bed, which was well recognizable as such, different outlines showed a slightly

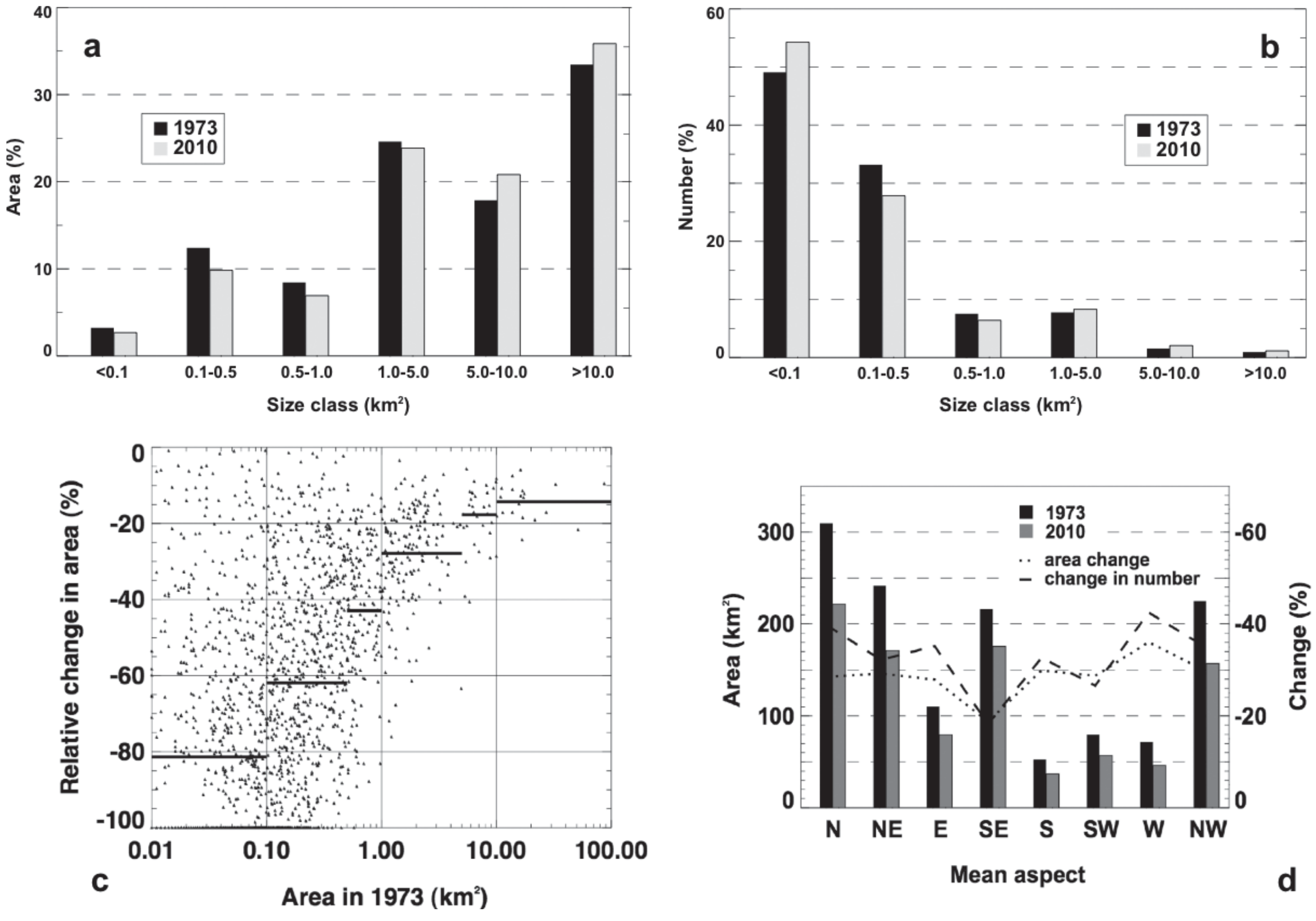

FIGURE 3. Percentages of (a) area and (b) number of glaciers for the entire Swiss Alps in 1973 and 2010 relative to the total. (c) Observed relative changes in area 1973–2010 versus initial area. Horizontal lines show average values for individual size classes. (d) Area distribution of glaciers in the entire Swiss Alps in 1973 and 2010 for classes of mean aspect and relative changes (%) in area and number.

inferior match but still remained quite constant (difference from 5 to 50 m, Fig. 4, parts b, c, and d). On the other hand, differences in mapped glacier extents were significantly larger among individual experts (from 5 to 200 m) if the following situations applied: (1) ambiguous differentiation between snow-covered glacier ice and seasonal and/or perennial snowfields (Fig. 4, parts d and e), or (2) ambiguous differentiation between debris-covered glacier ice and periglacial phenomena (e.g., rock glaciers) or ice-free scree/debris close to the glacier margin (Fig. 4, parts d and f). These qualitative observations are confirmed with statistical analyses summarized in Table 2. Mean percentaged standard deviation (STD) of total glacier area is significantly higher for glaciers with less clear glacier margins (10.1% for Glacier de Tortin [TOR], 11.1% for Vadret dal Corvatsch-S [COR], 17.9% for Gurschenfirn [GUR]; Fig. 4, parts d–f) than for glaciers with nearly clear-cut borders (2.0% for Vadret da Gueglia-S [GUE], 5.0% for Schwarzbachfirn [SWZ], 3.3% for St. Annafirn [STA]; Fig. 4, parts a–c).

When comparing the results of our accuracy assessment for very small glaciers with those by Paul et al. (2013), who applied the same methods to a larger data set, the resulting ranges of observed standard deviations or relative differences in delineated glacier area were found to be in good agreement (Fig. 5). In addition, our findings were also consistent with Paul et al. (2003), showing that relative area differences generally increase with decreasing glacier size—that is, that the relative accuracy of manual digitization of glacier outlines generally decreases toward very small glaciers. Nevertheless, we found that if high-resolution airborne or satellite imagery is used, relative differences and thus the relative accuracy of mapped glacier area is at the lower end of the overall uncertainty range even for smallest glaciers in case of good visibility and clear/distinct glacier margins (lower left in Fig. 5).

REASSESSING OUTLINES WITH DInSAR COHERENCE IMAGES

The terminus of Weingartengletscher-S-II in the Mischabel test area (0.78 km² in 1973, 0.42 km² in 2010) is heavily debris-covered (Fig. 6, part a). It is a good example of a glacier for which the manual delineation on the basis of visible interpretation of the aerial orthoimagery only was particularly difficult. The potential of more accurate mapping of partially or entirely debris-covered glaciers using DInSAR techniques becomes obvious in Figure 6, part b. Areas of distinct regular noise could be distinguished as a result of strongly decorrelated radar signals on the interferograms. This was caused by (1) the exposure of the melting ice itself (in case of rather thin debris-coverage), (2) the rapid settlement of the glacier surface, and/or (3) a significant glacier motion (Delaloye et al., 2007). We argue that the latter two caused the noise in the orographic upper-left part of the glacier still visible on the selected coherence image. For the

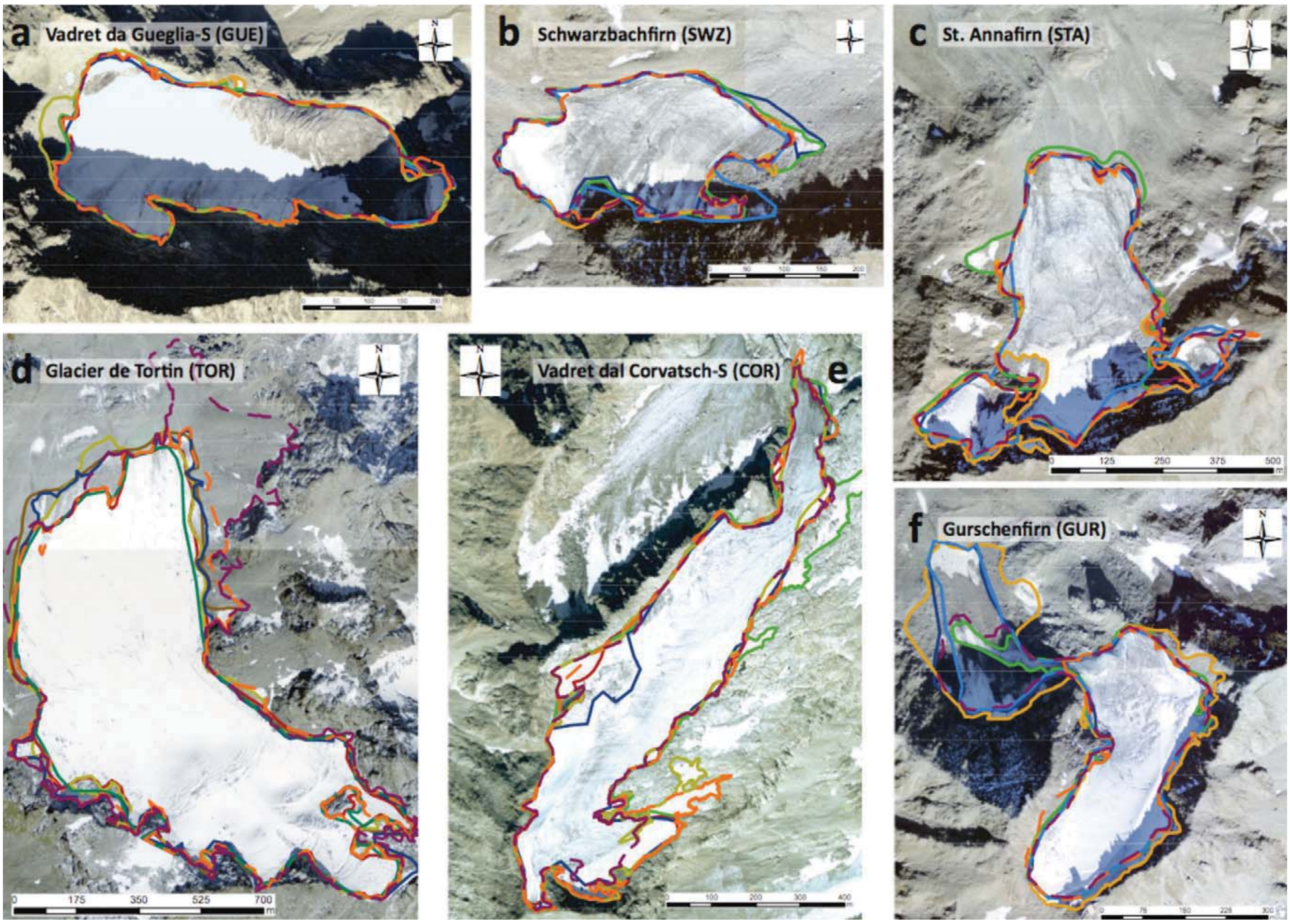

FIGURE 4. Overlays of outlines for six glaciers manually digitized by seven experts. Underlain are the SWISSIMAGE Level 2 orthophotos (25 cm resolution) from 2009 and 2010, which were used to delineate glacier boundaries. Locations of corresponding individual glaciers within the Swiss Alps are visible in Figure 1.

TABLE 2

Comparison of glacier area values derived from multiple digitization of glacier entities by different experts. The number of participants per glacier is given in parentheses. Glacier abbreviations are explained in the text.

Glacier	Area mean (km^2)	Area min (km^2)	Area max (km^2)	STD (%)
GUE (7)	0.103	0.101	0.107	2.0
SWZ (7)	0.052	0.050	0.053	5.0
STA (7)	0.207	0.196	0.213	3.3
TOR (7)	0.702	0.645	0.825	10.1
COR (7)	0.243	0.214	0.281	11.1
GUR (7)	0.114	0.083	0.150	17.9

lower-lying and sharply confined pattern that is still within the former 1973 glacier outlines, (1) and (3) could to a large extent explain the noise. From this we inferred that for Weingartengletscher-S-II, a rather large and highly debris-covered part of the current glacier tongue was misclassified as not belonging to the glacier anymore based on our digitization approach (Fig. 6).

We performed the comparison of the SGI2010 outlines with the outlines reassessed according to the respective coherence images for a subsample of 48 glaciers in the Mischabel area (Fig. 1) containing all size classes and surface types present in the Swiss Alps. The results showed that the example of Weingartengletscher-S-II (Fig. 6) was rather at the upper end of possible misclassification of debris-covered glacier ice (Fig. 7). The total area of the 48 glaciers mapped based on the aerial orthophotos was 78.8 km^2, whereas the refinement of glacier outlines using DInSAR techniques resulted in 81.7 km^2 (+2.9 km^2, or +3.7%). Reassessing the SGI2010 outlines for the Mischabel test area with DInSAR coherence images always resulted in an increase of the mapped glacier surface. Thus, there was a systematic bias in the SGI2010 for debris-covered glaciers. Furthermore, a trend of increasing scatter of the specific difference with decreasing glacier size could be observed (Fig. 7). Very small glaciers tended to be either almost entirely debris-covered or made up of almost only bare ice.

COMPARISON TO MEDIUM-RESOLUTION SOURCE DATA

In contrast to the shortcomings of semi-automatic glacier mapping techniques using medium-resolution satellite imagery (cf. Racoviteanu et al., 2009) and the difficulty of mapping very small glaciers based on such approaches in particular (e.g., Paul et al.,

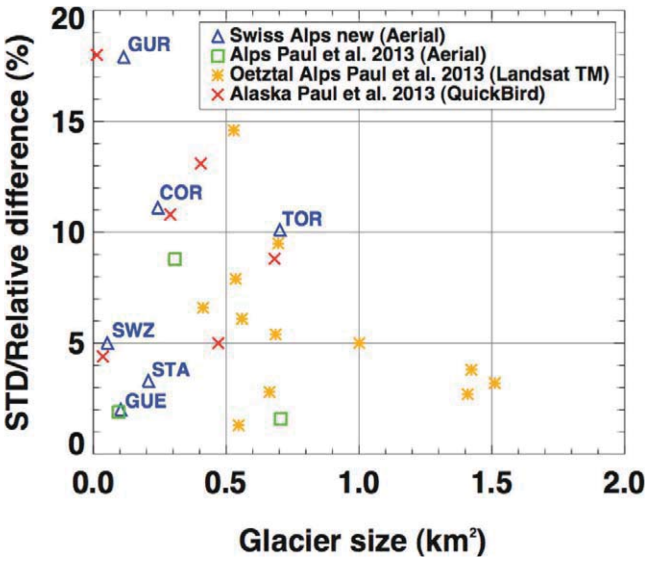

FIGURE 5. Glacier area versus standard deviation/relative difference of the manually digitized area values for several glaciers in Alaska and the European Alps according to Paul et al. (2013), and for the six very small glaciers in the Swiss Alps.

2013), the 25 cm aerial orthoimagery used here allowed accurate glacier mapping even for very small glaciers or for generally error-prone areas like cast shadow (Fig. 8). Glacier boundaries of the entire eastern Swiss Alps (CHeast, Fig. 1) were also mapped from SWISSIMAGE Level 1 orthophotographs acquired in September 2003. Therefore, we could directly compare our outlines with the 2003 inventory of the entire European Alps, for which the Landsat TM scenes were acquired on 6 August 2003 for the eastern Swiss Alps (Paul et al., 2011). For glaciers larger than 1.0 km^2, mapped glacier areas were nearly identical from both approaches. They tended to be a few percent larger for semi-automatically derived outlines (slightly positive biases; see Fig. 9). For glaciers smaller than 1.0 km^2, though, the difference and scatter significantly increased with every next smaller size class, both toward under- and overestimation of glacier area by Paul et al. (2011).

Within the eastern Swiss Alps, the 2003 inventory by Paul et al. (2011) comprised many glacier polygons of only one single or a few 30 × 30 m pixels. Often, these areas could be identified as tiny snow patches on the aerial orthophotographs. As a result, far fewer individual glacier polygons were mapped based on digitization from aerial orthoimages than from the semi-automatic mapping using medium-resolution satellite imagery. The minimum area mapped and still considered as an ice patch was larger, the largest glacier polygon (Morteratschgletscher) as well as the total glacierized area smaller compared to the satellite remote sensing outlines (Table 3). For individual glacier entities, a clear trend of increasing scatter toward decreasing glacier size class resulted from comparison of both methods. If we assume our outlines to be more accurate than those by Paul et al. (2011), this indicates that the accuracy of glacier outlines mapped with medium-resolution satellite remote sensing imagery significantly decreases toward smaller or smallest glaciers (Fig. 9). The spatial intersection of the 2003 CHeast outlines from both approaches showed that for very small glaciers (<0.5 km^2), more than 25% (>9.9 km^2) of the total area mapped by Paul et al. (2011) was misclassified, that is, was mapped as glacier-covered where no glacier ice could be distinguished based on the SWISSIMAGE orthophotographs (Table 3).

Discussion

GLACIER CHANGES 1973–2010

The total area change of –362.6 km^2 derived for all glaciers in the entire Swiss Alps between 1973 and 2010 (–27.7%, or –0.75% a^{-1} referred to the initial area) is in the range of values reported for other regions in the European Alps over the last decades. Glacier shrinkage observed by Diolaiuti et al. (2012) in the Aosta Valley, Western Italian Alps, is –44.3 km^2 (–27.0%, or –0.90% a^{-1}) between 1975 and 2005, in whole South Tyrol, Eastern Italian Alps, –43.2 km^2 (–31.6%, or –1.37% a^{-1}) within 1983 and 2006 (Knoll and Kerschner, 2009), and in the Ortles-Cevedale group –23.5 km^2 (–23.4%, or –1.06% a^{-1}) during 1987–2009 (Carturan et al., 2013). Glaciers in the Ötztal Alps (Austria) lost 28.1 km^2 (–19.5%, or –0.53% a^{-1}) between 1969 and 2006 (Abermann et al., 2009). For the entire European Alps, Paul et al. (2011) reported a total area loss of 859.1 km^2 (–29.5%, or –0.89% a^{-1}) over the period 1970(±15 a)–2003.

We note that direct comparison of such numbers can be critical for various reasons, such as diverse sample size or size class distribution of the investigated glaciers, different subregional to local climate conditions, various length and onset of observation periods, and so on. For Switzerland, for instance, from 1973 to 1985, the observed area change is only –1%. Between 1985 and 1999, the area loss rate increased and glaciers in the Swiss Alps lost 18% (1.3% a^{-1}) of their initial area (Paul et al., 2004). Together with our updated results, this gives a more detailed picture of glacier area changes: during the period of constant glacier recession between 1985 and 2010, we find an area change rate of –1.1% a^{-1}. Furthermore, for glaciers in the eastern Swiss Alps (CHeast, Fig. 1), both relative area losses and annual loss rates were highest for very small glaciers and lowest for the largest size class between 1973 and 2009 (Fig. 3, part c). Due to the similar size class distribution and abundance of glacier types, this subsample of glaciers can be regarded as representative for the entire Swiss or even European Alps. Splitting the observation period in two parts, we observe that annual loss rates of size classes >0.5 km^2 tended to increase between 2003–2009 compared to 1973–2003, whereas observed area changes showed a decreasing retreat rate for very small glaciers. Overall, annual area changes were more negative for the second observation period (Table 4). This would be in agreement with more negative glacier mass balances observed in the Swiss Alps since the mid-1980s (Huss et al., 2010; Fischer et al., 2014) and with projected future evolution of mass balance for different size classes (Huss, 2012). Similar to for instance the recent changes of very small glaciers in the Monashee Mountains, British Columbia, Canada (DeBeer and Sharp, 2009), the future evolution of very small glaciers in the Swiss Alps might be more strongly influenced by local topoclimatic factors than by the regional climatic forcing.

ACCURACY ASSESSMENT

We follow the recommendations by Paul et al. (2013) and assess the accuracy of outlines mapped based on our approach with an independent experiment on multiple digitization of clean, snow-, and/or debris-covered glaciers due to the lack of reference or ground truth data. We confirm that the accuracy of glacier extents derived from whatever glacier mapping technique generally decreases toward smallest glaciers. Nevertheless, we show that if high-resolution airborne or satellite remote sensing imagery is used, the uncertainty of mapped glacier area is—at least for clean glaciers and distinct glacier margins—at the lower end of the overall uncertainty range

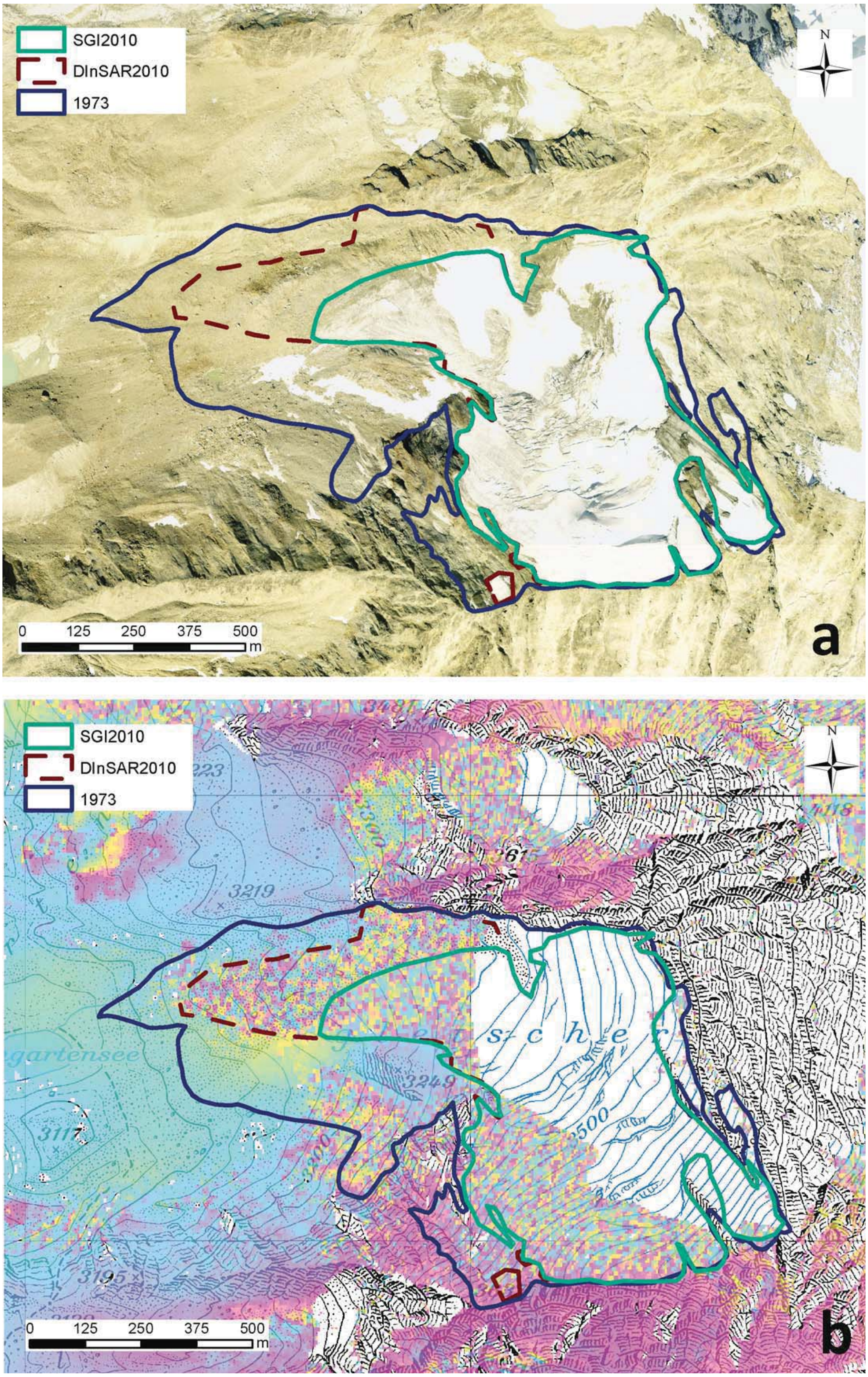

FIGURE 6. Outlines of Weingartengletscher-S-II in 1973 (navy blue), 2010 reassessed with DInSAR (dashed red), and original 2010 (green). Underlain is (a) the SWISSIMAGE Level 2 orthophoto acquired in autumn 2010, and (b) the TSX 11 days DInSAR scenes from 9–20 September 2010 in combination with the topographic pixelmap.

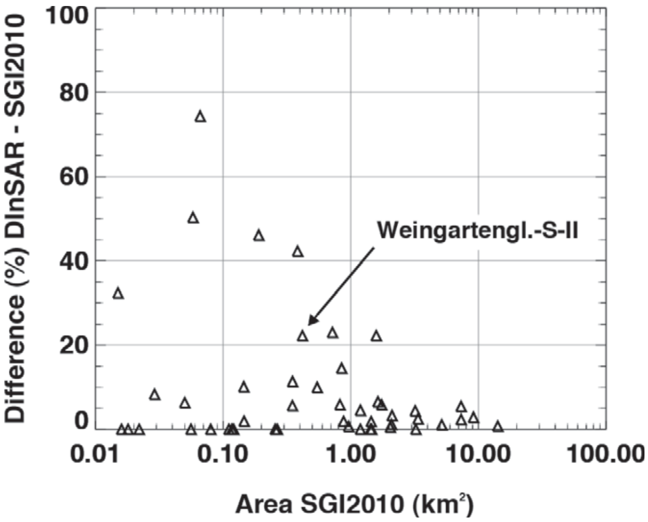

FIGURE 7. Relative difference between glacier outlines derived from combination of DInSAR interferograms and aerial orthophotos and glacier outlines derived from aerial orthophotos only versus glacier area 2010 for 48 individual glaciers in the Mischabel test region (Fig. 1).

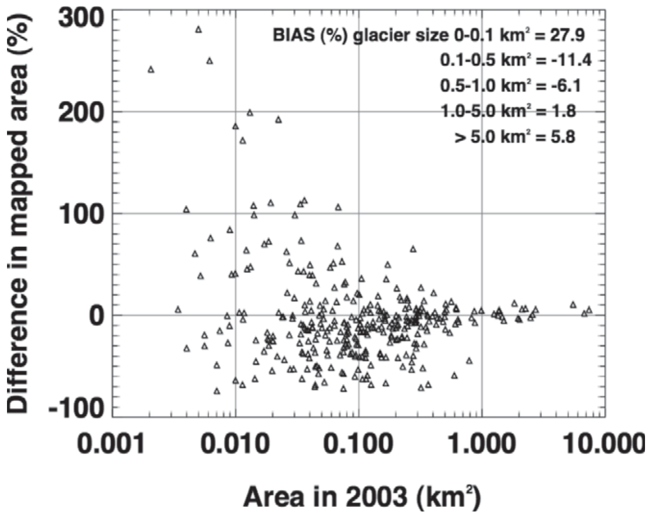

FIGURE 9. Differences in 2003 glacier areas in the eastern Swiss Alps between those derived from semi-automated methods using medium-resolution satellite remote sensing imagery (Paul et al., 2011) and those manually outlined from high-resolution aerial photographs (this study).

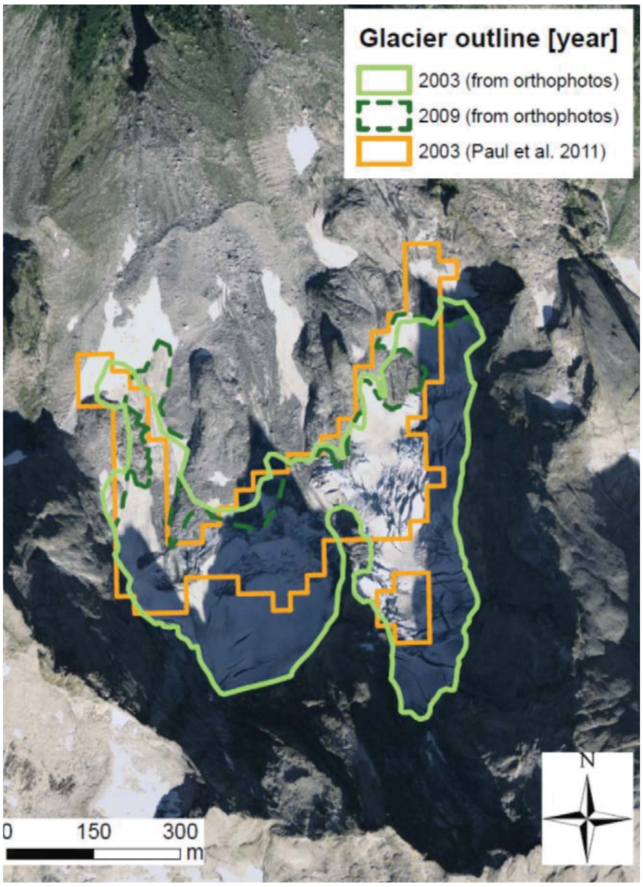

FIGURE 8. Different glacier outlines for Vadrec da la Trubinasca-E (0.22 km² in 2009): 2003 (light green) and 2009 (dashed dark green) from manual digitizing of high-resolution orthoimages, 2003 (orange) derived by semi-automatic satellite remote sensing (Paul et al., 2011). Underlain is the SWISSIMAGE Level 2 tile from autumn 2009.

TABLE 3

Comparison of glacier area values for 412 individual glaciers derived from manual digitization of high-resolution aerial orthophotographs (CHeast 2003) to those from medium-resolution satellite remote sensing imagery (Paul et al., 2011).

	CHeast 2003	Paul et al. (2011)
Number of polygons	418	1138
Min. area (km²)	2.1×10^{-3}	3×10^{-6}
Max. area (km²)	15.2	15.7
Total mapped area (km²)	160.1	165.8
Area of glaciers <0.5 km²	39.7 km²	28.9 km²

TABLE 4

Changes in area of glaciers in the eastern Swiss Alps 1973–2003/2009 evaluated for different size classes.

Size class (km²)	1973 area (km²)	2003 area (km²)	2009 area (km²)	Change 1973–2003 (% a^{-1})	Change 2003–2009 (% a^{-1})
<0.1	12.0	8.2	7.7	–1.1	–0.8
0.1–0.5	58.5	31.5	28.0	–1.5	–1.0
0.5–1.0	34.4	20.9	14.4	–1.3	–3.2
1.0–5.0	75.6	46.0	41.1	–1.3	–1.1
>5.0	60.5	53.5	51.0	–0.4	–0.7
Total	241.0	160.1	142.2	–1.1	–1.3

even for very small glaciers. For glaciers larger than 1.0 km², we learn from comparison of both approaches that semi-automatic glacier mapping mostly produces nearly identical outlines as manual digitization does. Therefore, we argue that the accuracy of these methods is also comparable for glacier size classes >1.0 km^2 and is thus less than ±5% of the total mapped area (cf. Paul et al., 2013). If we consider our 2003 outlines mapped for the eastern Swiss Alps as one large single "round robin" experiment on multiple digitization per se, we are able to quantify the accuracy of our approach to ±4.7% of the area for glaciers between 1.0 and 5.0 km^2, and to ±3.1% of the area for glaciers larger than 5.0 km^2 (Fig. 9). From the average value of standard deviations observed for all glaciers smaller than 1.0 km^2 (Fig. 5), we quantify the accuracy to ±7.6% for mapped areas of these smallest size classes. Consecutively, the accuracy of the total area mapped in the SGI2010 (944.3 km^2) is calculated from these size class dependent accuracies as ±24.1 km^2.

From the combination of aerial orthophotography data with DInSAR scenes of shortest time lapse we can reassess our outlines for debris-covered glaciers within the Mischabel test region. This always results in an increase in mapped glacier surface. Thus, if we consider the delineation of glacier outlines from a combination of aerial orthophotographs and DInSAR techniques to be more accurate than our methodological approach chosen for the entire Swiss Alps for the creation of the SGI2010, the error of mapping debris-covered glaciers is a systematic one and increases again steadily toward smallest glaciers. From the representative subsample of the Mischabel test area we can quantify this error to +3.7% of the mapped area. This indicates that the total glacierized area in the Swiss Alps might be slightly underestimated by the SGI2010. The same probably also applies to the former 1973 inventory and, hence, does not affect the 1973–2010 area change assessments as errors would cancel each other out.

HIGH-RESOLUTION SOURCE DATA FOR GLACIER MAPPING

Semi-automatic satellite remote sensing approaches are well established and widely used today. Without the benefits of spaceborne glacier mapping methods, for instance, the recently compiled Randolph Glacier Inventory (RGI) containing outlines of all glaciers and ice caps around the globe (cf. Pfeffer et al., 2014) and consecutive global-scale modeling approaches (e.g., Huss and Farinotti, 2012; Radić et al., 2013) would not have been feasible. Nevertheless, with our study we show that if medium-resolution satellite imagery is used (e.g., from Landsat or ASTER), remote sensing techniques may not provide the accuracy of glacier outlines needed to allow proper change assessments for small and very small glaciers. By direct and glacier-individual comparison of the former 2003 glacier outlines derived by Paul et al. (2011) to our glacier extents created by manual digitization from aerial orthophotographs of 2003, we quantitatively demonstrate to what extent outlines of small and very small glaciers created from medium-resolution imagery can deviate from those mapped from higher resolution source data (Fig. 9 and Table 3). Overall, we find that for glaciers smaller than 0.5 km^2, more than 25% in area are erroneously mapped as glacierized if medium-resolution source data are used. Extrapolating these findings to the entire Swiss Alps would imply that more than 30 out of 118 km^2 would have been misclassified as glacier-covered (Table 1).

Using high-resolution source data works in favor of accurate glacier mapping because it provides a high level of visible detail and small-scale structures like crevasses, exposed glacier ice below snow or debris-cover, or abrupt changes in the surface topography. Together with the absence of clouds and the favorable snow conditions, the 25 cm aerial SWISSIMAGE orthoimagery used here is particularly valuable for the compilation of the SGI2010. Over highly debris-covered areas, however, glacier outlines cannot be digitized without doubt, even based on high-resolution source data. The availability of a former glacier inventory can help avoid missing any glacierized surfaces or erroneously mapping seasonal and/or perennial snow as glacier-covered. Furthermore, it allows adoption of the nomenclature and coding scheme, which facilitates the change assessment for individual glacier entities. Although for many parts of the world snow conditions may not be as favorable as in Switzerland and source data of comparable quality might be lacking, we recommend using source data of highest possible quality and resolution for future creation of glacier inventories in areas dominated by very small glaciers such as the European Alps, the Rocky Mountains, and the Southern Alps of New Zealand.

Recently, different authors applied new tools for automatic or semi-automatic delineation of glacier outlines using source data of higher quality and resolution. With the aim of creating a new glacier inventory, though, such approaches have proven not (yet) to be applicable to the entire Swiss Alps for various reasons. Knoll and Kerschner (2009) used and improved an automatic algorithm by Kodde et al. (2007) to generate a glacier inventory for South Tyrol, Italy, applying classification criterions such as topographical smoothness, connectivity, hydrological constraints, and geomorphometrical parameters. For very small glaciers, however, even the improved algorithm did not yield sufficient accuracy, and outlines had to be corrected manually with digital orthophotos (Knoll and Kerschner, 2009). Abermann et al. (2009, 2010) used surface elevation changes and shaded reliefs from multitemporal high-resolution digital elevation models (DEMs) derived by airborne laser scanning (ALS) surveys of the Ötztal and Stubai Alps, Austria. They report promising results and high accuracy even for the delineation of very small glaciers. Limiting factors of this method are high costs as well as—at least today—low spatio-temporal coverage of such high-resolution ALS source data. Trying to apply approaches mentioned above by Knoll and Kerschner (2009) or Abermann et al. (2009, 2010) might have helped to further improve the accuracy of our inventory. Nonetheless, we show that the quality of the digital orthoimagery used for creation of the SGI2010 still today legitimates the benefit of the considerable effort that manual delineation of glacier outlines for the entire Swiss Alps required.

Conclusions

We have presented the new Swiss Glacier Inventory SGI2010 derived from manual delineation of glacier outlines based on high-resolution (25 cm) aerial orthophotographs acquired between 2008 and 2011. Unlike the two previous inventories of 2000 and 2003 created by semi-automatic approaches using medium-resolution satellite remote sensing imagery, we strictly coded and named outlines for individual glacier entities according to the hydrologically based coding system of the former 1973 inventory (Müller et al., 1976; Maisch et al., 2000). This allowed glacier-individual change assessments over the 37-year period of 1973–2010. Within the entire Swiss Alps, the total glacierized area mapped for 2010 is 944.3 ±24.1 km^2 (–27.7%, or –0.75% a^{-1} since 1973). On average, relative area changes between 1973 and 2010 were highest for smallest glaciers and decreased toward largest glacier size classes. Further, an amplification of the dominance in number of very small glaciers (<0.5 km^2) was observed. In contrast to the general trend toward increasingly negative area changes, area loss rates decreased for very small glaciers in the eastern Swiss Alps between 2003–2009 compared to 1973–2003.

The accuracy of the SGI2010 was assessed by comparison of extents for clean, snow-, and/or debris-covered glaciers derived from multiple digitization by different experts. The resulting uncertainty was less than ±5% of the mapped area for glaciers >1.0 km^2 but generally increased toward smallest glaciers.

We demonstrated that the combination of aerial orthophotographs with Differential SAR Interferometry techniques is promising to map debris-covered glaciers more precisely. Using coherence images from selected TerraSAR-X DInSAR pairs, we reassessed glacier outlines of a test area where visual interpretation based on the high-resolution orthophotographs only was difficult. From comparison of these refined outlines to those of the SGI2010 we could quantify the error of debris-covered glaciers to +3.7%.

For the eastern Swiss Alps, glacier outlines were mapped twice, once for the SGI2010 based on the most recent and once based on the 2003 aerial orthophotographs. From the direct comparison to the 2003 inventory derived by Paul et al. (2011) we learned that for glaciers >1.0 km^2, comparable results could be achieved with both approaches. For glaciers <1.0 km^2, though, the uncertainty and errors of glacier mapping with medium-resolution (30 m) satellite remote sensing techniques significantly increased with every next smaller size class. The investigated semi-automatic remote sensing approach misclassified more than 25% in area of very small glaciers in the eastern Swiss Alps. For these size classes, glacier extents mapped from high-resolution (25 cm) aerial orthophotographs provided better accuracy.

The use of high-resolution source data for glacier mapping implies a high level of visible detail and structure, which is in advantage of producing accurate outlines even for the smallest glacier size classes. Good contrast, the absence of clouds and favorable snow conditions on air- or spaceborne high-resolution imagery can further improve the accuracy of derived glacier boundaries. Correct mapping of highly debris-covered areas remains challenging even if high-resolution source data are used. Nevertheless, we recommend use of source data with highest possible resolution and quality for future creation of glacier inventories in areas dominated by very small glaciers such as the European Alps.

Acknowledgments

This study is supported by the Swiss National Science Foundation (SNSF), grant 200021_137586. The SWISSIMAGE and swissALTI^{3D} data sets were purchased from the Swiss Federal Office of Topography (swisstopo), license no. 5704003629. The Deutsches Zentrum für Luft- und Raumfahrt (DLR) provided us with the TerraSAR-X (TSX) DInSAR pairs (projects LAN 411 and LAN 1145) and the University of Zurich (UZH) with the 1973 and 2003 glacier inventories in digital format. Special thanks to all the different experts for providing us with individual glacier outlines for the accuracy assessment, and to B. H. Raup for transferring the data set into the GLIMS database. Comments by F. Paul, a second anonymous reviewer, and the scientific editor H. Jiskoot were helpful to finalize the paper.

References Cited

Abermann, J., Lambrecht, A., Fischer, A., and Kuhn, M., 2009: Quantifying changes and trends in glacier area and volume in the Austrian Ötztal Alps (1969–1997–2006). *The Cryosphere*, 3: 205–215.

Abermann, J., Fischer, A., Lambrecht, A., and Geist, T., 2010: On the potential of very high-resolution repeat DEMs in glacial and periglacial environments. *The Cryosphere*, 4: 53–65.

Andreassen, L. M., and Winsvold, S. H. (eds.), 2012: *Inventory of Norwegian Glaciers*. Oslo: NVE Rapport 38, 236 pp.

Atwood, D. K., Meyer, F., and Arendt, A., 2010: Using L-band SAR coherence to delineate glacier extent. *Canadian Journal of Remote Sensing*, 36(1): 186–195.

Bahr, D. B., and Radić, V., 2012: Significant contribution to total mass from very small glaciers. *The Cryosphere*, 6: 763–770.

Bolch, T., Menounos, B., and Wheate, R., 2010: Landsat-based inventory of glaciers in western Canada, 1985–2005. *Remote Sensing of Environment*, 114(1): 127–137.

Carturan, L., Filippi, R., Seppi, R., Gabrielli, P., Notarnicola, C., Bertoldi, L., Paul, F., Rastner, P., Cazorzi, F., Dinale, R., and Dalla Fontana, G., 2013: Area and volume loss of the glaciers in the Ortles-Cevedale group (Eastern Italian Alps): controls and imbalance of the remaining glaciers. *The Cryosphere*, 7: 267–319.

DeBeer, C., and Sharp, M., 2009: Topographic influences on recent changes of very small glaciers in the Monashee Mountains, British Columbia, Canada. *Journal of Glaciology*, 55: 691–700.

Delaloye, R., Lambiel, C., Lugon, R., Raetzo, H., and Strozzi, T., 2007: Typical ERS InSAR signature of slope movement in a periglacial mountain environment (Swiss Alps). *Proceedings of the ENVISAT Symposium 2007*, July 2007, Montreux, Switzerland, ESA SP-636.

Diolaiuti, G. A., Bocchiola, D., Vagliasindi, M., D'Agata, C., and Smiraglia, C., 2012: The 1975–2005 glacier changes in Aosta Valley (Italy) and the relations with climate evolution. *Progress in Physical Geography*, 36(6): 764–785.

Evans, I. S., 2006: Glacier distribution in the Alps: statistical modelling of altitude and aspect. *Geografiska Annaler: Series A, Physical Geography,* 88(2): 115–133.

Evans, I. S., and Cox, N. J., 2005: Global variations of local asymmetry in glacier altitude: separation of north-south and east-west components. *Journal of Glaciology*, 51(174): 469–482.

Falaschi, D., Bravo, C., Masiokas, M., Villalba, R., and Rivera, A., 2013: First glacier inventory and recent changes in glacier area in the Monte San Lorenzo region (47°S), Southern Patagonian Andes, South America. *Arctic, Antarctic, and Alpine Research*, 45(1): 19–28.

Farinotti, D., Huss, M., Bauder, A., and Funk, M., 2009: An estimate of the glacier ice volume in the Swiss Alps. *Global and Planetary Change*, 68: 225–231.

Fischer, M., Huss, M., and Hoelzle, M., 2014: Surface elevation and mass changes of all Swiss glaciers 1980–2010. *The Cryosphere Discussion*, 8: 4581–4617, doi: http://dx.doi.org/10.5194/tcd-8-4581-2014.

Frey, H., Paul, F., and Strozzi, T., 2012: Compilation of a glacier inventory for the western Himalayas from satellite data: methods, challenges and results. *Remote Sensing of Environment*, 124: 832–843.

Glaciological Reports, 2011–2014: *The Swiss Glaciers, 2007/08–2010/11*. Yearbooks of the Cryospheric Commission of the Swiss Academy of Sciences (SCNAT), No. 129/130. Published since 1964 by the Laboratory of Hydraulics, Hydrology and Glaciology (VAW) of the ETH Zurich.

Haeberli, W., 2004: Glaciers and ice caps: historical background and strategies of worldwide monitoring. *In* Bamber, J. L., and Payne, A. J. (eds.), *Mass Balance of the Cryosphere*. Cambridge, UK: Cambridge University Press, 559–578.

Haeberli, W., and Hoelzle, M., 1995: Application of inventory data for estimating characteristics of and regional climate-change effects on mountain glaciers: a pilot study with the European Alps. *Annals of Glaciology*, 21: 206–212.

Hoelzle, M., Chinn, T. J., Stumm, D., Paul, F., Zemp, M., and Haeberli, W., 2007: The application of inventory data for estimating characteristics of and regional past climate-change effects on mountain glaciers: a comparison between the European Alps and the New Zealand Alps. *Global and Planetary Change*, 56: 69–82.

Huss, M., 2010: Mass balance of Pizolgletscher. *Geographica Helvetica*, 65(2): 80–91.

Huss, M., 2011: Present and future contribution of glaciers to runoff from macroscale drainage basins in Europe. *Water Resources Research*, 47: W07511, http://dx.doi.org/10.1029/2010WR010299.

Huss, M., 2012: Extrapolating glacier mass balance series to the mountain-range scale: The European Alps 1900–2100. *The Cryosphere*, 6: 713–729.

Huss, M., and Farinotti, D., 2012: Distributed ice thickness and volume of all glaciers around the globe. *Journal of Geophysical Research*, 117: F04010, http://dx.doi.org/10.1029/2012JF002523.

Huss, M., Hock, R., Bauder, A., and Funk, M., 2010: 100-year mass changes in the Swiss Alps linked to the Atlantic Multidecadal Oscillation. *Geophysical Research Letters*, 37(10): L10501, http://dx.doi.org/10.1029/2010GL042616.

IPCC, 2013: *Climate Change 2013. The Physical Science Basis.* Working Group I Contribution to the Fifth Assessment Report of the Intergovernmental Panel on Climate Change, WMO/UNEP, Cambridge University Press.

Ivy-Ochs, S., Kerschner, H., Maisch, M., Christl, M., Kubik, P. W., and Schlüchter, C., 2009: Latest Pleistocene and Holocene glacier variations in the European Alps. *Quaternary Science Reviews*, 28: 2137–2149, doi:10.1016/j.quascirev.2009.03.009.

Klees, R., and Massonnet, D., 1999: Deformation measurements using SAR interferometry: potential and limitations. *Geologie en Mijnbouw*, 77: 161–176.

Knoll, C., and Kerschner, H., 2009: A glacier inventory for South Tyrol, Italy, based on airborne laser-scanner data. *Annals of Glaciology*, 50(53): 46–52.

Kodde, M., Pfeifer, N., Gorte, B., Geist, T., and Höfle, B., 2007: Automatic glacier surface analysis from airborne laser scanning. *International Archives of the Photogrammetry, Remote Sensing and Spatial Information Sciences*, 36 (3/W52): 221–226.

Lambrecht, A., and Kuhn, M., 2007: Glacier changes in the Austrian Alps during the last three decades, derived from the new Austrian glacier inventory. *Annals of Glaciology*, 46: 177–184.

Machguth, H., and Huss, M., 2014: The length of the world's glaciers—a new approach for the global calculation of center lines. *The Cryosphere*, 8: 1741–1755.

Maisch, M., Wipf, A., Denneler, B., Battaglia, J., and Benz, C., 2000: *Die Gletscher der Schweizer Alpen: Gletscherhochstand 1850, Aktuelle Vergletscherung, Gletscherschwundszenarien. Schlussbericht NFP 31*. Second edition. Zurich: vdf Hochschulverlag ETH Zurich, 373 p.

Massonnet, D., and Feigl, K. L., 1998: Radar interferometry and its application to changes in the Earth's surface. *Reviews of Geophysics*, 36: 441–500.

Müller, F., Caflish, T., and Müller, G., 1976: *Firn und Eis der Schweizer Alpen, Gletscherinventar*. Zurich: vdf Hochschulverlag ETH Zurich, 224 p.

Nuth, C., Kohler, J., König, M., von Deschwanden, A., Hagen, J. O., Kääb, A., Moholdt, G., and Pettersson, R., 2013: Decadal changes from a multi-temporal glacier inventory of Svalbard. *The Cryosphere*, 7: 1603–1621.

Paul, F., 2004: The new Swiss glacier inventory 2000: *Application of Remote Sensing and GIS*. Ph.D. thesis, Department of Geography, University of Zurich, 198 pp.

Paul, F., Kääb, A., and Haeberli, W., 2007: Recent glacier changes in the Alps observed by satellite: consequences for future monitoring strategies. *Global and Planetary Change*, 56: 111–122.

Paul, F., Kääb, A., Maisch, M., Kellenberger, T. W., and Haeberli, W., 2002: The new remote-sensing-derived Swiss glacier inventory: I. Methods. *Annals of Glaciology*, 34: 355–361.

Paul, F., Huggel, C., Kääb, A., Kellenberger, T., and Maisch, M., 2003: Comparison of TM-derived glacier areas with higher resolution data sets. *EARSeL eProceedings*, 2(1): 15–21.

Paul, F., Kääb, A., Maisch, M., Kellenberger, T., and Haeberli, W., 2004: Rapid disintegration of Alpine glaciers observed with satellite data. *Geophysical Research Letters*, 31: L21402, http://dx.doi.org/10.1029/2004GL020816.

Paul, F., Barry, R., Cogley, G., Frey, H., Haeberli, W., Ohmura, A., Ommanney, S., Raup, B., Rivera, A., and Zemp, M., 2009: Recommendations for the compilation of glacier inventory data from digital sources. *Annals of Glaciology*, 51(53): 119–126.

Paul, F., Frey, H., and LeBris, R., 2011: A new glacier inventory for the European Alps from Landsat TM scenes of 2003: challenges and results. *Annals of Glaciology*, 52(59): 144–152.

Paul, F., Barrand, N. E., Baumann, S., Berthier, E., Bolch, T., Casey, K., Frey, H., Joshi, S. P., Konovalov, V., LeBris, R., Mölg, N., Nosenko, G., Nuth, C., Pope, A., Racoviteanu, A., Rastner, P., Raup, B., Scharrer, K., Steffen, S., and Winsvold, S., 2013: On the accuracy of glacier outlines derived from remote-sensing data. *Annals of Glaciology*, 54(63): 171–182.

Pfeffer, W. T., Arendt, A. A., Bliss, A., Bolch, T., Cogley, J. G., Gardner, A. S., Hagen, J. O., Hock, R., Kaser, G., Kienholz, C., Miles, E. S., Moholdt, G., Mölg, N., Paul, F., Radić, V., Rastner, P., Raup, B. H., Rich, J., Sharp, M. J., and the Randolph Consortium, 2014: The Randolph Glacier Inventory: a globally complete inventory of glaciers. *Journal of Glaciology*, 60(221), 537–552.

Racoviteanu, A. E., Paul, F., Raup, B., Khalsa, S. J. S., and Armstrong, R., 2009: Challenges and recommendations in mapping of glacier parameters from space: results of the 2008 Global Land Ice Measurements from Space (GLIMS) workshop, Boulder, Colorado, USA. *Annals of Glaciology*, 50(53): 53–69.

Radić, V., Bliss, A., Beedlow, A. C., Hock, R., Miles, E. and Cogley, J. G., 2013: Regional and global projections of twenty-first century glacier mass changes in response to climate scenarios from global climate models. *Climate Dynamics*, http://dx.doi.org/10.1007/s00382-013-1719-7.

Raup, B., Kääb, A., Kargel, J. S., Bishop, M. P., Hamilton, G., Lee, E., Paul, F., Soltesz, D., Khalsa, S. J. S., Beedle, M., and Helm, C., 2007: Remote sensing and GIS technology in the Global Land Ice Measurement from Space (GLIMS) Project. *Computers and Geosciences*, 33: 104–125.

Sorg, A., Bolch, T., Stoffel, M., Solomina, O., and Beniston, M., 2012: Climate change impacts on glaciers and runoff in Tien Shan (Central Asia). *Nature Climate Change*, 2: 725–731.

Strozzi, T., Wegmüller, U., and Matzler, C., 1999: Mapping wet snow covers with SAR interferometry. *International Journal of Remote Sensing*, 20: 2397–2403.

Strozzi, T., Paul, F., and Kääb, A., 2010: Glacier mapping with ALOS PALSAR within the GlobGlacier project. *Proceedings of the ESA Living Planet Symposium 2010*, 28 June–2 July 2010, Bergen, Norway.

swisstopo, 2010: Swiss Federal Office of Topography, SWISSIMAGE. Das digitale Farborthophotomosaik der Schweiz, http://www.swisstopo.admin.ch/internet/swisstopo/de/home/products/images/ortho/swissimage.parsysrelated1.76752.downloadList.50684.DownloadFile.tmp/infosi201003deu.pdf, accessed 20 December 2013.

swisstopo, 2013: Swiss Federal Office of Topography, swissALTI^{3D}. Ausgabebericht 2013, http://www.swisstopo.admin.ch/internet/swisstopo/de/home/products/height/swissALTI3D/swissALTI3D.parsys.13145.downloadList.74256.DownloadFile.tmp/swissalti3drelease2013de.pdf, accessed 20 December 2013.

Weydahl, D. J., 2001: Analysis of ERS Tandem SAR coherence from glaciers, valleys and fjord ice on Svalbard. *IEEE Transactions on Geoscience and Remote Sensing*, 39(9): 2029–2039.

Zemp, M., Paul, F., Hoelzle, M., and Haeberli, W., 2008: Glacier fluctuations in the European Alps 1850–2000: an overview and spatio-temporal analysis of available data. *In* Orlove, B., Wiegandt, E., and Luckman, E. H. (eds.), *Darkening Peaks: Glacier Retreat, Science, and Society*. Berkeley: University of California Press, 152–167.

Zemp, M., Frey, H., Gärtner-Roer, I., Nussbaumer, S. U., Hoelzle, M., Paul, F., and Haeberli, W. (eds.), 2012: *Fluctuations of Glaciers 2005–2010, Volume X*. ICSU (WDS)/IUGG (IACS)/UNEP/UNESCO/WMO, World Glacier Monitoring Service, Zurich, Switzerland, 336 pp. Publication based on database version: http://dx.doi.org/10.5904/wgms-fog-2012-11.

Zemp, M., Nussbaumer, S. U., Naegeli, K., Gärtner-Roer, I., Paul, F., Hoelzle, M., and Haeberli, W. (eds.), 2013: *Glacier Mass Balance Bulletin No. 12 (2010–2011)*. ICSU (WDS)/IUGG (IACS)/UNEP/UNESCO/WMO, World Glacier Monitoring Service, Zurich, Switzerland, 106 pp. Publication based on database version: http://dx.doi.org/10.5904/wgms-fog-2013-11.